Peer-reviewed version available at *Hydrology* **2018**, *5*, 17; doi:10.3390/hydrology5010017

Article

Thermal Regime of a Temperate Deep Lake and Its Response to Climate Change: Lake Kuttara, Japan

Kazuhisa A. Chikita [1,*], Hideo Oyagi [2], Tadao Aiyama [3], Misao Okada [4], Hideyuki Sakamoto [5] and Toshihisa Itaya [6]

[1] Arctic Research Center, Hokkaido University; chikita@sci.hokudai.ac.jp
[2] College of Humanities and Sciences, Nihon University 2; oyagi.hideo@nihon-u.ac.jp
[3] The Fukuda Hydrology Center, Inc. 3; aiyama.chitose@gmail.com
[4] Suiko-Research, Inc. 4; okadax@suiko-r.co.jp
[5] Hokkaido Brown Bear Museum 5; sakamoto@bearpark.jp
[6] Shin Engineering Consultant, Inc. 6; itaya-t@indigo.plala.or.jp
* Correspondence: chikita@sci.hokudai.ac.jp; Tel.: +81-11-706-2764

Abstract: A temperate deep lake, Lake Kuttara, Hokkaido, Japan (148 m deep at maximum) was completely frozen every winter in the 20th century. However, unfrozen conditions of the lake over winter occurred four times in the 21st century, which is probably due to global warming. In order to understand how thermal regime of the lake responds to climate change, its heat storage change was calculated by estimating heat budget of the lake and monitoring water temperature at the deepest point for September 2012–June 2016. As a result, temporal change of the heat storage from the heat budget was very consistent with that from the direct temperature measurement (determination coefficient R^2 = 0.827). The 1978–2017 data at a meteorological station near Kuttara indicated that there are significant (less than 5% level) long-term trends for air temperature (0.024 °C/yr) and wind speed (−0.010 m/s/yr). A sensitivity analysis for the heat storage from the heat budget estimate and an estimate of return periods for mean air temperature in mid-winter allow us to conclude that the lake could be unfrozen once per about two year in a decade.

Keywords: non-freezing; temperate lake; heat budget; heat storage; global warming

---

1. Introduction

At present, global warming tends to increase unfrozen days in the arctic to subarctic regions [1,2], though a temporal slowdown in the global warming in 1998- 2013 was reported [3,4]. Following the Köppen-Geiger climate classification, the Hokkaido Island, Japan, belongs to the southernmost subarctic area, where some water regions increase unfrozen days [2]. Two deep caldera lakes, Shikotsu (360.1 m deep at maximum) and Toya (180.0 m deep at maximum), Hokkaido, are known as secularly unfrozen lakes [5-7]. Two curators, Ms. Naoko Mayeda and Mr. Hideyuki Sakamoto, of the Bear Museum at site B (Figure 1) have been observing daily freezing conditions of Lake Kuttara since 1980's. According to their report, Lake Kuttara (148.0 m deep at maximum), located between Shikotsu and Toya, was completely frozen in the 20th century, when ice-ridge lines were often built up [8]. However, Kuttara was completely unfrozen in 2004, 2007 and 2009, and partly frozen only one day in 2015, due to relatively warm winters. Even if frozen, the lake tends to shorten the frozen periods [9]. Non-freezing or shortening frozen periods could affect the aquatic ecosystem, because the solar radiation input then increases and nutrient input by snowmelt and rainfall runoffs from the surrounding catchment slope occurs at any time.

How lakes are frozen and then the lake ice is grown is physically developed by Ashton [10], Aihara et al. [8], Gebre et al. [11] and Leppäranta [12]. Aihara et al. [8] simulated the ice growth in Lake Kuttara by applying a three-layered model of snow, snow ice and pure ice. Applying a

Preprints (www.preprints.org) | NOT PEER-REVIEWED | Posted: 2 January 2018 doi:10.20944/preprints201801.0005.v1

Peer-reviewed version available at Hydrology 2018, 5, 17; doi:10.3390/hydrology5010017

one-dimensional multi-year model, MyLake, of Saloranta and Andersen [13], Gebre et al. [11] simulated lake ice phenology and annual maximum lake ice thickness in the Nordic region. The Nordic lakes are completely frozen in November – May, while Lake Kuttara is frozen in late January – mid-April at longest and was completely unfrozen in 2004, 2007 and 2009, and partly frozen in 2015. Kuttara is thus suitable for the investigation of a critical thermal condition for freeze or non-freeze over winter. In this study, heat budget of temperate Lake Kuttara is estimated for about 4 years, and the calculated heat storage change is compared with observed one from moored temperature loggers. An increase in the frequency of unfrozen conditions for the future is predicted from significant long-term trends for air temperature and wind speed.

2. Study Area and Observations

A temperate deep lake, Lake Kuttara (42°29′57″ N, 141°10′55″ E; lake level, ca. 258 m above sea level abbreviated as "asl"; 4.68 km^2 in area), was formed 40,000 years ago by the volcanic eruption of Kuttara Volcano (Figure 1). Three lakes, Kuttara, Shikotsu and Toya, are located in the Shikotsu-Toya National Park designated in May 1949. The lakes have been seriously preserved from land development, though Toya suffered from water pollution by drainage from mines in 1939 - 1973. Kuttara is topographically closed, since it has no outflowing river. However, the lake is hydrologically open because groundwater outflow is estimated at 0.44 m^3/s [14]. This outflow corresponds to a decrease in lake level at 7.6 mm/day. Kuttara is dimictic, where vertical circulations occur twice per year (in late December and early to late April, when the lake is thermally uniform at about 4 °C).

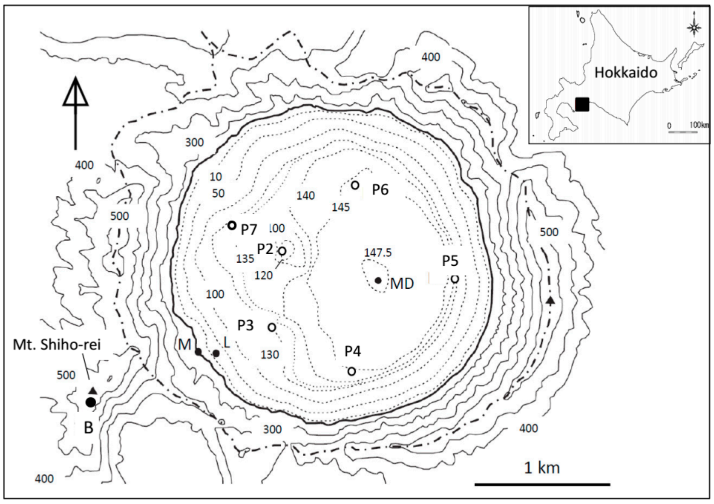

Figure 1. Location mas of Lake Kuttara, Hokkaido, Japan, and observation sites on the bathymetric map of the lake.

In order to estimate heat storage change of Lake Kuttara, 33 temperature data loggers were moored at the deepest point (site MD in Figure 1) on 1 September 2012 (Figure 2). The data loggers deployed are 20 Stowaway TidbiT, eight HOBO TidbiT v2 and five HOBO Pro v2 (accuracy, ±0.2 °C; Onset Computer, Inc., USA), which record water temperature at 30 min intervals. Since the accuracy of the temperature loggers is relatively low, they were calibrated by a standard thermometer (accuracy, ±0.02 °C) and a RINKO-profiler (model ASTD102, JFE Advantec, Inc., Japan; accuracy, ±0.01 °C) at a range of 0 – 35 °C. Meanwhile, the lake level seasonally varies with the amplitude of less than ca. 1.5 m. The mooring system in Figure 2 thus provides the depth-overlapping measurement of water temperature by the lowest four or five loggers below the surface marker buoy and the uppermost two loggers (140 m and 142 m above bottom) below the underwater buoy. Vertical profiles (0.1 m pitch) of water temperature from the profiler were obtained once per two month on average at seven sites, MD and P2 – P7 during the loggers' mooring (1 September 2012 –

Peer-reviewed version available at Hydrology 2018, 5, 17; doi:10.3390/hydrology5010017

30 June 2016). The profiler needs 15 to 26 minutes to get a vertical profile at each of 7 sites, and totally about 4 hrs to get vertical profiles at all the sites in the unfrozen periods.

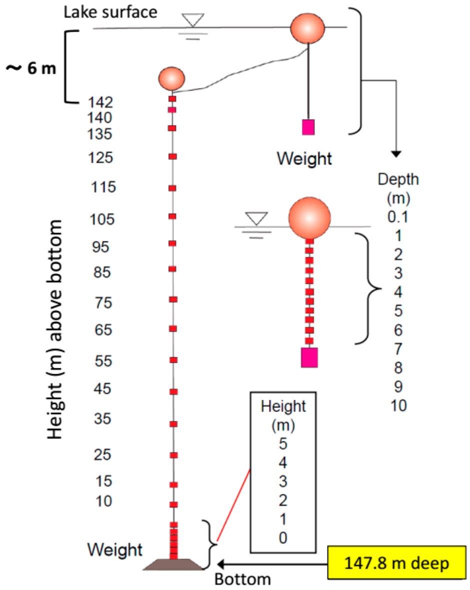

Figure 2. Mooring system of temperature loggers at site MD.

Meteorology (solar radiation, air temperature, relative humidity, rainfall, air pressure and wind velocity) at the lake was observed at 30 min intervals at site M (ca. 3 m above the lake level), and water level at 30 min intervals at site L (Figure 1). Meteorology for data-missing periods was complemented from the linear relationship with data of AMeDAS (Automated Meteorological Data Acquisition System) Noboribetsu station (42°27′30″ N, 141°7′6″ E; 197 m asl) at 5.7 km southwest of site M and the Muroran Meteorological Observatory (42°18′42″ N, 140°58′30″ E; 39.9 m asl) at 25.8 km southwest of site M (correlation coefficient r = 0.852, 0.912, 0.805, 0.987, 0.995 and 0.734 for wind speed, air pressure, solar radiation, precipitation, air temperature and relative humidity, respectively; $p < 0.01$). For snowfall and snow depth on the lake shore, the Noboribetsu data were utilized, assuming that the northern winter monsoon, producing snowfall, blows similarly at both Lake Kuttara and Noboribetsu. Rainfall or snowfall in winter was judged by air temperature and relative humidity at site M.

The lake level at site L was obtained at 30 min interval from a pressure data logger (model U20-001-01, HOBO Water Level Data Logger, Onset Computer Inc., USA; accuracy, ±0.3% FS for a range of 0 – 207 kPa) and air pressure at site M. Here, the calculated water depth (m) at site L was correlated with the lake level (m asl) from frequent topographic surveys, referring to the 1st class benchmark (no. H17-1-19; 42°29′35.2264″ N, 141°10′13.8119″ E; 263.682 m asl) of Geospatial Information Authority of Japan near site M. As a result, the observation error of lake level was about ±0.01 m. The lake level data are utilized at the daily mean base in the estimate of heat budget of the lake. Then, the effect of small and short surface oscillations such as surface seiche, wind wave, etc. can be neglected [15].

Inflow of some perennial streams is seen around site M. Their amount and water temperature were frequently measured in February to October. The non-freeze, partial freeze or complete freeze of Lake Kuttara in winter has been judged by Mr. H. Sakamoto or Ms. M. Maeda, a curator of the Bear Museum at site B since 1980's. As a result, the lake was completely frozen in the winters of 2013, 2014 and 2016, but partially frozen only one day in the winter of 2015. The thickness and inner structure of lake ice and upper snow after complete freeze were examined at site MD on 19 March 2013 and 21 February 2014.

Preprints (www.preprints.org) | NOT PEER-REVIEWED | Posted: 2 January 2018 doi:10.20944/preprints201801.0005.v1

Peer-reviewed version available at *Hydrology* **2018**, *5*, 17; doi:10.3390/hydrology5010017

3. Observational Results and Discussion

Figure 3 shows time series of daily mean air temperature and solar radiation, and daily mean water level (m asl) and daily precipitation for 2 September 2012 – 30 June 2016. The lake level varied with the amplitude of ca. 1.5 m, increasing in response to rainfalls, especially those in autumn. The increasing rate of lake level responding to rainfall is about 0.06 m per 50 mm/day. During relatively small rainfall at less than 10 mm/day or non-rainfall, the lake level decreases consistently. This is caused by the net groundwater output (groundwater outflow, ca. 0.4 m^3/s) rather than evaporation at water surface [14]. When the day of 1st May is adopted as the first day of a hydrological year for the lake, the three years of 1 May 2013 – 30 April 2014, 1 May 2014 – 30 April 2015 and 1 May 2015 – 30 April 2016 showed total precipitation at 2,182 mm (rainfall 93.6 %, snowfall 6.4 %), 2,143.5 mm (rainfall 95.0 %, snowfall 5.0 %) and 1,665 mm (rainfall 93.9 %, snowfall 6.1 %), respectively. As a result, the relatively small rainfalls in the final year induced very small fluctuations of lake level (Figure 3), when the rainfalls are likely balanced by the net groundwater output. Stream inflow near site M was totally less than 0.01 m^3/s at water temperature of 3 – 23 °C.

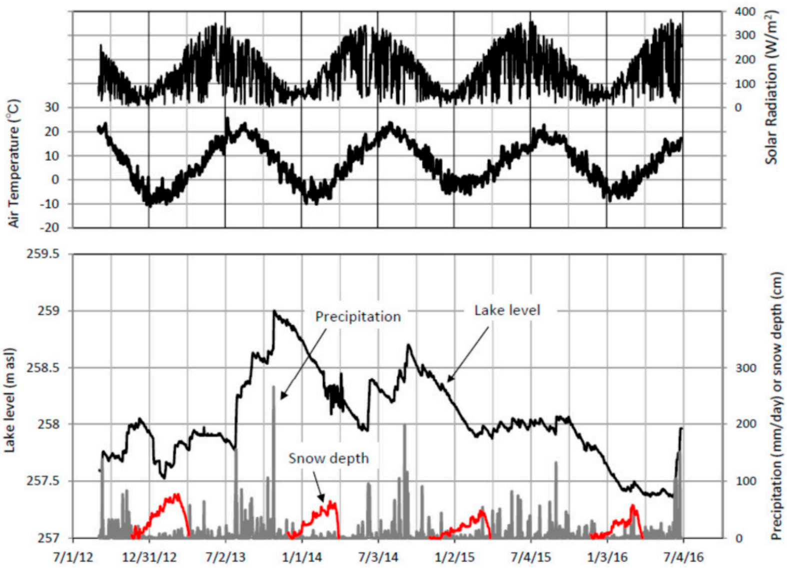

Figure 3. Temporal variations of meteorology and lake level.

Air temperature averaged over 1 December - 28 or 29 February was -5.6 °C in Dec. 2012 – Feb. 2013, -3.5 °C in Dec. 2013 – Feb. 2014, -1.4 °C in Dec. 2014 – Feb. 2015 and -2.7 °C in Dec. 2015 – Feb. 2016. Meanwhile, the lake was completely frozen for 82 days (25 January – 16 April) in 2013, 57 days (8 February – 5 April) in 2014, and 31 days (23 February – 24 March) in 2016, and partially frozen (70 % area) only for one day (12 January 2015). Thus, frozen conditions of the lake are likely controlled by the winter temperatures, where -1.4 °C in 2015 seems to be critical for freeze or non-freeze (i.e., unfrozen at more than -1.4 °C). Before complete freeze, negative air temperature occurred for 50 days between 19 November 2012 and 25 January 2013, for 56 days between 28 November 2013 and 8 February 2014, for 39 days between 14 November 2014 and 12 January 2015 (partially frozen), and for 69 days between 22 November 2015 and 23 February 2016. Mean air temperature over these four periods was -4.3 °C, -3.2 °C, -1.4 °C and -2.2 °C, respectively. Thus, mean air temperature (here, -1.4 °C) for the days with negative air temperature before complete or partial freeze could also be one of meteorological factors determining freeze or non-freeze. The number of days with negative air temperature before complete freeze is smallest (50 days) in the winter of 2012 - 2013, but the mean air temperature was then lowest at -4.3 °C. Hence, it is seen that the efficiency of cooling down to complete freeze was highest in 2012 – 2013. Observations at site B offered freezing processes in the lake by two ways; one is pure-ice extension from lake shore by natural cooling, and the other is snowy-ice formation from relatively large snowfall onto water surface. In the latter way, the lake was completely frozen in about a day.

Peer-reviewed version available at Hydrology 2018, 5, 17; doi:10.3390/hydrology5010017

Figure 4 shows vertical distributions (0.1 m pitch) of water temperature at site MD in February 2015 – May 2016. The T_{md} line depicts water temperature (°C) giving maximum density under water pressure and salinity at a certain water depth **[6],** and, in case of Lake Kuttara, 3.69 °C at 148.0 m. Lake Kuttara was partially frozen only on 12 January 2015, and completely frozen for 23 February – 24 March 2016. Thus, the temperature profiles of 20 February 2015 and 19 February and 21 May 2016 in Figure 4 have no 0 °C layers at surface because of no ice. On 20 February 2015, the surface temperature was ca. 2 °C with the ca. 4 °C layer at depths of more than 100 m. Thus, the lake was thermally stratified even under completely unfrozen condition. It is seen that, at depths of more than 90 m, the temporal change of water temperature is less than 1 °C. During the intense stratification of June - August, the bottom temperature at 3.86 °C (6 June 2015) increased up to 4.07 °C (29 August 2015). This suggests that relatively warm water including dissolved solids leaks from below the bottom [7]. In fact, a geophysical survey by the magnetotelluric (MT) method in the Kuttara caldera indicates that there is a reservoir of geothermal water below the bottom at the deepest point [18].

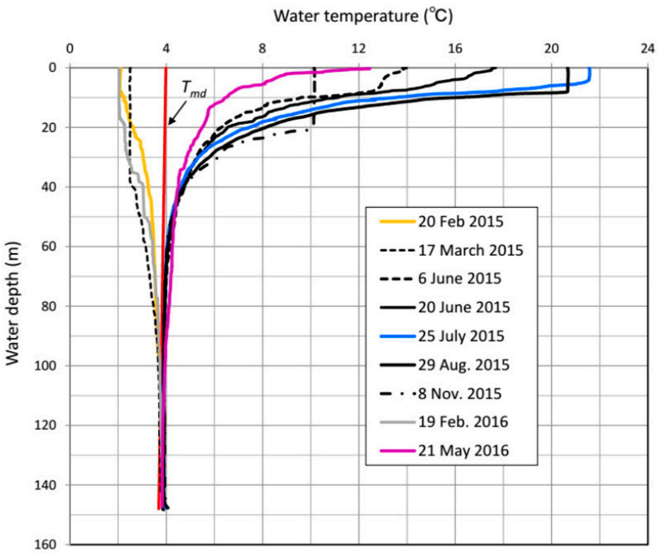

Figure 4. Vertical distributions of temperature T_{md}, giving maximum water density, and water temperature at site MD.

Figure 5 shows time series of daily mean water temperature from 0.2 m depth to the bottom (147.1 – 148.9 m in depth) for 2 September 2012 – 30 June 2016. The depths of more than 10 m are those averaged over the observed periods. The lake was completely frozen for 82 days in 2013, 57 days in 2014, and 31 days in 2016. It is seen that, as the frozen periods are longer, the water temperatures at 0.2m, 5 m and 12. 8 m approach to 0 °C. This means that the upper layer is cooled by downward growth of pure ice [8]. In 2015 partially frozen, water temperature at depths of 42.8 m or less changes very similarly at less than 4 °C. This indicates that the vertical mixing by wind is active over the winter. Thus, the investigation of the cooling process in a lake is needed to understand how the lake freezes and grows ice year by year. The snow and ice on 19 March 2013 were 0.51 m thick, being 0.08 m snow, 0.07 m pure ice, 0.03 m inter-layered water, 0.09m snowy ice and 0.24 m pure ice downward. The inter-layered water is probably part of rainwater and meltwater supplied on 13 March 2013 with daily mean air temperature of 1.77 °C and daily rainfall of 2 mm. The snow and ice on 21 February 2014 consisted of pure ice 0.30 m thick and the upper snow 0.10 m thick. Thus, it is seen that the 2014 freeze without snowy ice occurred by pure-ice extension from the lake shore.

Peer-reviewed version available at Hydrology 2018, 5, 17; doi:10.3390/hydrology5010017

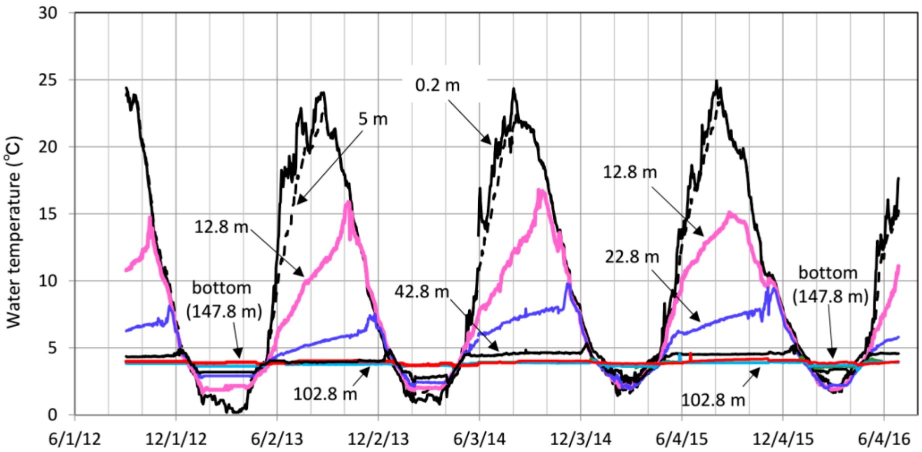

Figure 5. Temporal variations of daily mean water temperature at seven depths of site MD.

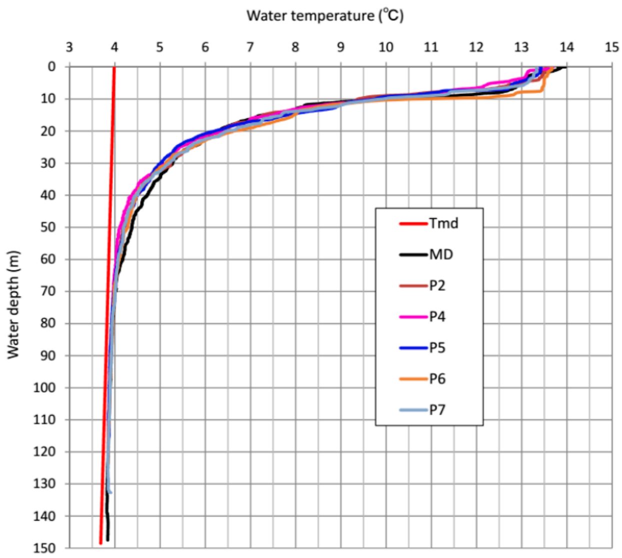

Figure 6. Vertical distributions of water temperature at six sites, P2 and P4 – P7 and MD with the T_{md} line.

Figure 6 shows vertical distributions of water temperature at six sites, MD and P2, P4 – P7 on 6 June 2015 (Figure 1). The temperature difference between the six profiles at a certain depth was ca. 1 °C at maximum. The small difference is due to both the small stream inflow (without prevalent river-induced currents) and active horizontal mixing by the sea wind in daily land-sea wind cycles or from episodic cyclones in the Pacific Ocean [15]. Here, the difference of ca. 1 °C is regarded as a maximum error in estimating heat storage changes of the lake from the daily mean temperature only at site MD (Figure 5). At depths of 70 – 140 m, the temperature at six sites is close to the T_{md} line. This suggests that the vertical circulation in spring occurred enough at these depths. At depths of 140 m, however, geothermal water leakage after the circulation seems to slightly increase the temperature, thus being a little far from the T_{md} value [19].

4. Heat Storage Change of the Lake

Here, the heat storage change of Lake Kuttara will be numerically obtained by two ways; by direct measurements of water temperature and water level, and by the heat budget estimate. The ways are connected by the following equation:

Peer-reviewed version available at *Hydrology* **2018**, *5*, 17; doi:10.3390/hydrology5010017

$$\Delta G/\Delta t = \left[\Delta\left[\int_{-h}^{0}\{\rho_w c_p T(z)\}\cdot A(z)dz\right]/\Delta t\right]/A_0$$
$$= R_n - Q_H - Q_E + Q_P + H_{Rin} + H_G + H_S \qquad (1)$$

where ΔG is heat storage change (J/m^2) of a lake for a budget period Δt (sec), h is water depth (m) at deepest point, ρ_w and c_p are water density (kg/m^3) and specific heat of water (J/kg/K) at temperature T (K), respectively, A is lake area (m^2) at a depth, z (m) ($A = A_0$ at lake surface, $z = 0$), R_n is net radiation (W/m^2), Q_H is sensible heat flux (W/m^2), Q_E is latent heat flux (W/m^2), Q_P is heat flux (W/m^2) by direct precipitation onto the lake, H_{Rin} is heat flux (W/m^2) by river inflow, H_G is heat flux (W/m^2) by net groundwater inflow, and H_s is heat flux (W/m^2) at lake bottom. H_{Rin}, H_G and Q_P in equation (1) are given as follows:

$$H_{Rin} = (\rho_w c_p R_{in} T_{Rin})/A_0 \qquad (2)$$

$$H_G = H_{Gin} - H_{Gout} = (\rho_w c_p G_{in} T_{Gin} - \rho_w c_p G_{out} T_{Gout})/A_0 \qquad (3)$$

$$Q_P = \rho_w c_p P T_p \qquad (4)$$

where R_{in} is river inflow (m^3/s), T_{Rin} is water temperature (K) of infloing rivers, G_{in} and G_{out} are groundwater inflow and outflow (m^3/s), H_{Gin} and H_{Gout} are heat fluxes (W/m^2) by groundwater inflow and outflow, respectively, T_{Gin} and T_{Gout} are temperatures (K) of inflowing and outflowing grounwaters, respectively, P is precipitation (m/s) onto lake surface, T_P is temperature (K) of precipitation (here, assumed to be equal to air temperature). Here, daily means of the meteorlogical factors, lake level and temperarues were utlized for a budget period, Δt = 86400 sec. In case of snowfall onto the lake, latent heat of ice from the negative air temperature to 0 °C and fusion heat of the 0 °C ice in water are reduced from equation (4). The heat flux, H_s, at lake bottom in equation (1) is here negleted, because it is of the order of 1 W/m^2 at the deepest point [19], thus being much smaller than the solar radition in Figure 3. H_{Rin} in equation (2) is less than 3 W/m^2, since R_{in} < 0.01 m^3/s and T_{Rin} = 276.15 – 296.15 K. Thus, H_{Rin} was also neglected.

Net radiation R_n in equation (1) consists of net shortwave radiation K^* and net longwave radiation L^*, as given by the following:

$$R_n = K^* + L^* = (1-\alpha)S_d + L_d - L_{up} = (1-\alpha)S_d + L_d - \varepsilon\sigma T_s^4 \qquad (5)$$

where S_d is downward shortwave radiation, α is albedo, L_d and L_{up} are downward and upward longwave radiations, respectively, ε is emissivity (here, 0.97 for ice (or snowy ice), water and snow, and 1.0 for air), σ is Stefan-Bolzman constant (=5.67×10^{-8} W/m^2/K^4), and T_s is surface water temperature (K). Referring to observational results of Brandt and Warren [20], α values of water, snow, ice (or snowy ice) and snowy water were given as constants of 0.05, 0.8, 0.5 and 0.3, respectively. The α values were then determined depending on lake surface conditions during freeze, i.e., pure-ice extension from lake shore, snowy water (slush) just after snowfall, snowy ice after its freeze and snow accumulation on ice. Downward longwave radiation L_d was numerically obtained as a function of air temperature, total amount of effective water vapor content and relative sunshine duration [21].

Sensible heat flux Q_H and latent heat flux Q_E in equation (1) was numerically obtained by the following bulk transfer method:

$$Q_H = (c\rho_a a_H u_z)\cdot(T_s - T_z) \qquad (6)$$

$$Q_E = lE = -l\left(\frac{\rho_a \beta}{p}\right)\cdot(a_E u_z)\cdot(e_z - e_0) \qquad (7)$$

where ρ_a is air density (=1.2 kg/m^3), c is specific heat (J/Kg/K) of air under constant pressure, β is ratio of water vapor density to dry air density (=0.622), a_H and a_E are dimensionless bulk transfer

Preprints (www.preprints.org) | NOT PEER-REVIEWED | Posted: 2 January 2018 doi:10.20944/preprints201801.0005.v1

Peer-reviewed version available at Hydrology 2018, 5, 17; doi:10.3390/hydrology5010017

coefficients for sensible heat and latent heat, respectively, u_z is wind speed (m/s) at z (m) above ground surface, T_z is air temperature (K) at z, T_s is surface temperature (K) at water surface, ice surface or snow surface, l is latent heat (J/kg) for evaporation, p is air pressure (Pa) at z, e_z is vapor pressure (Pa) at z, and e_0 is satuarated vapor pressure (Pa) at T_s. Assuming the atomospheric condition to be neutral at any time, $a_H = a_E$ ~$1.5 \cdot 10^{-3}$ was given for 1 ~ < u_3 < ~10 m/s [21]. During complete freeze, Q_E is zero at ice-water interface, but, instead, sublimation from ice or snow surface at less than 0 °C or evaporation at water surface of 0 °C (after rainfall) above ice surface was caluculated. At T_3 > 0 °C, T_s = 0 °C is given, and the net heat flux, $R_n - Q_H - Q_E + Q_P$, at surface is then consumed as fusion heat of ice or snow. When the right side of equation (1) was negative at ice-water interface after complete freeze, and also its absolute value is larger than the upward heat flux at ice-water interface, the consequent heat loss was replaced by pure-ice growth. Snow depth on ice after complete freeze was supposed to be equal to snow depth after the date of freeze at the Noboribetsu station.

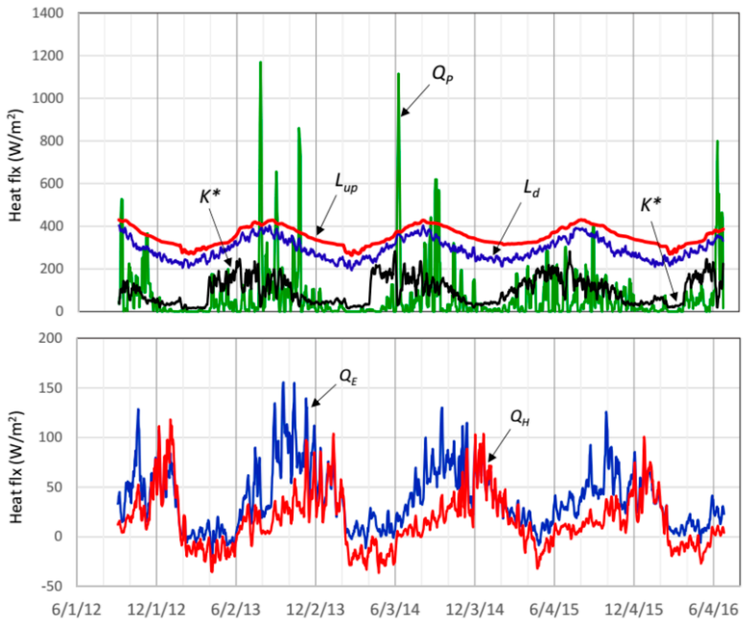

Figure 7. Temporal variations of six heat fluxes at lake surface (5-day moving average).

The integration of heat storage change between z = — h and 0 m in equation (1) was numerically obtained by water temperature of 0 – 90 m depth, because of little temperature fluctuaiton at depths of more than 90 m (Figure 4). Lake area A(z) was acquired at 5 m depth interval by using the bathymetric map published by Geospatial Information Authority of Japan.

5. Calculated Results

Figure 7 shows 5-day moving average for each of the thermal terms, K^*, L_{up}, L_d, Q_P, Q_H and Q_E at water surface, ice surface or snow surface. Depending on the albedo of water surface, ice surface and snow surface, net shortwave radiaition K^* changes greatly, especially for a time period of complete freeze to open water in early April or mid-April. Rainfalls at 25 mm/day or more (Figure 3) can effectively increase the heat storage change of the lake, since the heat flux Q_p is then at any time more than K^*. For the frozen period, Q_H is consistently negative, thus heating ice or snow surface. Then, the net heat flux H_G by groundwater input and output in equation (3) is estimated at -67 W/m² from G_{in} = 0.16 m³/s, G_{out}= 0.44 m³/s, T_{Gin} = 1 ℃ and T_{Gout} = 4 ℃ [14]. The value of – 67 W/m² corresponds to the annual minimum, since G_{in} tends to increase by rainfall. The calculated value, H_{Gout} = 110 W/m², for the frozen period is probably similar in the other seasons, since the change of lake level is small at ca. 1.5 m (Figure 3). In the frozen period, H_G = -67 W/m² is comparable in magnitude to the other heat terms. Thus, the net heat flux by groundwater input and output cannot

Preprints (www.preprints.org) | NOT PEER-REVIEWED | Posted: 2 January 2018 doi:10.20944/preprints201801.0005.v1

Peer-reviewed version available at Hydrology 2018, 5, 17; doi:10.3390/hydrology5010017

be neglected. A temporal change of H_G could induce the error in the heat budget estimate in equation (1). The heat flux H_s at lake bottom was of the order 1 W/m² [19], thus being negligible.

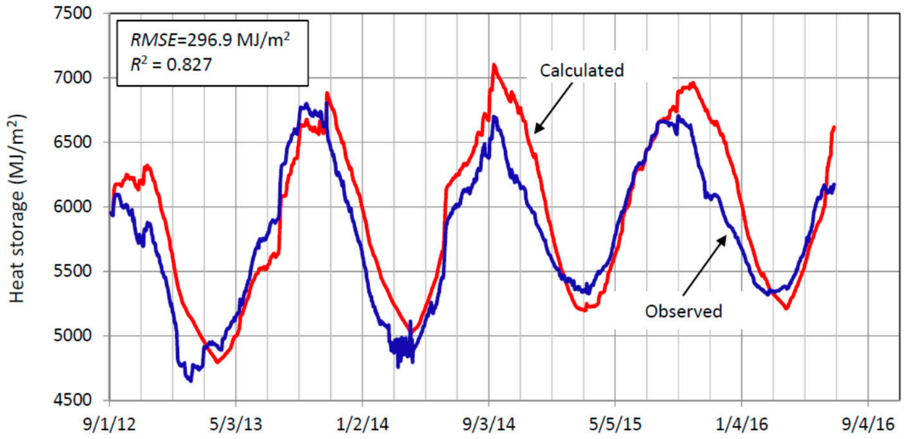

Figure 8. Temporal variations of observed and calculated heat storage.

Figure 8 shows temporal variations of observed and calculated heat storage G (J/m²). The observed heat storage change ΔG was obtained by the integration of water depth (-h, 0) in equation (1) from the water temperature measurement at site MD. In Figure 8, daily heat storage change ΔG is accumulated from the initial heat storage, 5.96×10³ MJ/m², of 2 September 2012 for the observation period. As a result, the calculated G from the heat budget estimate on the right side of equation (1) is reasonable to the observed one with the determination coefficient R^2=0.827 and the root-mean square error $RMSE$=296.9 MJ/m². The net heat flux H_G by groundwater input and output was then given as a constant of -49 W/m² to give the best fit to the observed G. Thus, temporal variation of daily heat storage can be reasonably acquired by data of meteorology, lake level and surface water temperature, though the parameter, H_G, contains some uncertainty. Here, R^2 and $RMSE$ are given as follows:

$$R^2 = 1 - \sum_{t=1}^{T}\left(G_0^t - G_{cal}^t\right)^2 / \sum_{t=1}^{T}\left(G_0^t - \overline{G_0}\right)^2 \quad (8)$$

$$RMSE = \left[\sum_{t=1}^{T}\left(G_0^t - G_{cal}^t\right)^2 / T\right]^{1/2} \quad (9)$$

where G_0^t and G_{cal}^t are observed and calculated heat storages on the t^{th} day, respectively, and $\overline{G_0}$ is heat storage averaged over the observation period T. The observed G in Figure 8 indicates that the lake receives heating in mid-February – mid-August and coolng in mid-August – mid-February. The calculated G tends to be overestimated as a whole. This is probably due to overestimation of H_G (= -49 W/m²) in the relatively cold winters of 2013 and 2014, since H_G = - 67 W/m² is obtained in a frozen period as a minimum throughout the year [14]. It is needed to know how H_{Gin} and H_{Gout} change seasonally. In the winter of 2015, the lake was partly frozen only one day (12 January). Thus, this winter could provide a critical heat storage for non-freezing. As a result, the observed G gives G = 5.35×10³ MJ/m² as the lowest heat storage for non-freeze. The lowest G in 2013, 2014 and 2016 was 4.66×10³ MJ/m², 4.85×10³ MJ/m² and 5.32×10³ MJ/m²., thus corresponding to the durations of complete freeze, 82 days, 57 days and 31 days, respectively.

6. Prediction for Non-Freezing

By sensitivity analysis for the calculated heat storage, Chikita et al. [22] revealed that the heat storage of Lake Kuttara increases effectively with increasing air temperature and rainfall. Applying the 1978 – 2017data of the Noboribetsu meteorological station, it is found that there are statistically

Preprints (www.preprints.org) | NOT PEER-REVIEWED | Posted: 2 January 2018 doi:10.20944/preprints201801.0005.v1

Peer-reviewed version available at Hydrology 2018, 5, 17; doi:10.3390/hydrology5010017

siginificant long-term trends (less than 5 % level) for annual mean air temperature and wind speed. As a result, an increasing rate of air temperature was given at +0.024 ℃/yr, and a decreasing rate of wind speed, at -0.01 m/s/yr. Meanwhile, annual rainfall and precipitation did not dipict any siginificant trends. Assuming the trends to be equal to those at the lake, it is possible to predict changes of heat storage and non-freezing conditions for the future.

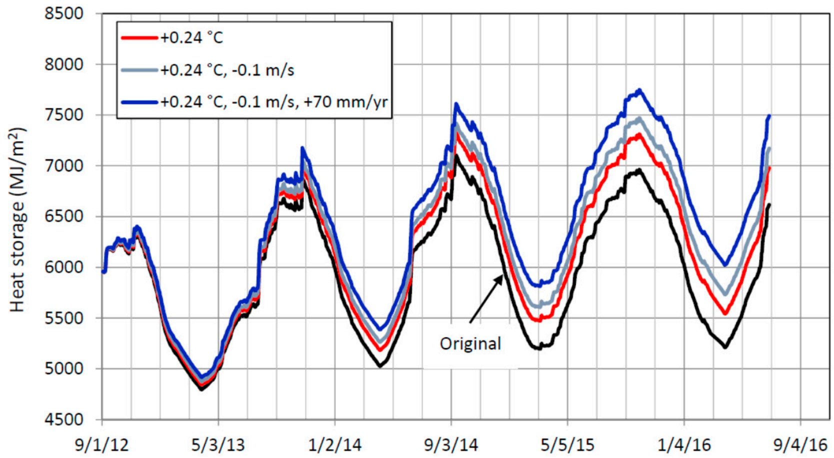

Figure 9. Temporal variations of calculated heat storage responding to air temperature at +0.24 °C, wind speed at -0.1 m/s and annual rainfall at +70 mm.

Figure 9 shows temporal variations of heat storage *G* calculated under condition of air temperature at +0.24 °C, wind speed at -0.1 m/s and annual rainfall at +70 mm. These values are equivalent to annual mean air temperature and wind speed in a decade, and σ/4 of the 40-yr annual rainfall (σ, standard deviaiton). As a result, the increase of +0.24 °C increases the lowest heat storage in 2014 up to the critical heat storage in 2015, and its combination with -0.1 m/s provides heat storage more than the critical value. When the annual rainfall at + 70 mm is added, the heat storage increases more greatly. In the 40-yr Noboribetsu data, the return period of mean air temperature in Decmeber – February is 2.2 years and 4.1 years for Dec. 2013 – Feb. 2014 and Dec. 2014 – Feb. 2015, respectively. Thus, in a decade, the unfrozen condition could occur every ca. 2 yr on average from every ca. 4 yr at present. A return period of mean air temperature in Dec. 2012 – Feb. 2013 was 10.3 yrs. Thus, if the lowest heat storage in 2013 approches to the critical level, $G = 5.35\times10^3$ MJ/m², for the future, Lake Kuttara may be secularly unfrozen.

7. Conclusions

Data of meteorology, lake level and water temperature for the period of 2 September 2012 – 30 June 2016 were obtained for Lake Kuttara, and its heat storage change ΔG was estimated by two ways, i.e., ΔG_0 from direct water temperature measurement and ΔG_{cal} from the heat budget estimate. In the winter of 2015, the lake is partly frozen only one day, while, in the winters of 2013, 2014 and 2016, it was completely frozen. The lowest heat storage of 5.35×10^3 MJ/m² in the 2015 winter can thus be a critical heat storage for non-freeze. Giving the net heat flux H_G by groundwater input and output at a constant of - 47 W/m², the temporal variation of heat storage G_{cal} is consistent with that of G_0, showing R^2=0.827 and *RMSE*=296.9 MJ/m². However, the H_G value could change in response to rainfall, since H_G = -67 W/m² in the frozen period is given as the annual miminum. It is needed to know how groundwater input G_{in} and groundwater output G_{out} temporally change in the water budget. Based on sensitivity analysis for heat storage G_{cal}, non-freezing of the lake for the future was discussed. Significant long-term trends from the 40-yr meteorologcal data indicate +0.024 °C/yr for air temperature and -0.01 m/s/yr for wind speed. As a result, the air temperatue at + 0.24 °C and its combination with the wind speed at -0.1 m/s increase the heat storage up to the non-freeze level.

Peer-reviewed version available at *Hydrology* **2018**, *5*, 17; doi:10.3390/hydrology5010017

Considering returen periods of mean air temperature in the winters, in a decade, the non-freeze of the lake could occur every ca. 2 yr from every ca. 4 yr at present.

Acknowledgments: We are indebted to Mr. T. Okudera for his great help of our field observations in Lake Kuttara. Dr. N. Kanna and Mr. T. Ozawa, Arctic Research Center, Hokkaido University, helped us keep the mooring system over the years. The Fukuda Hydrology Center, Ltd., Sapporo, kindly provided a snowmobile for our winter observations.

References

1. Magnuson, J. J. et al. Historical trends in lake and river ice cover in the Northern Hemisphere. *Science*, **2000**, 289, 1743-1746.
2. Kim Y.; Kimball J.S.; Zhang K.; McDonald, K.C. Satellite detection of increasing Northern Hemisphere non-frozen seasons from 1979 to 2008: Implications for regional vegetation growth. *Remote Sensing of Environment*, **2012**, 121, 472–487.
3. IPCC, *Climate Change 2013*. The Physical Science Basis. Contribution of Working Group I to the Fifth Assessment Report of the Intergovernmental Panel on Climate Change, 2013, Cambridge Univ. Press, Cambridge, U. K, 1535 pp.
4. Yan, X.-H.; Boyer, T.; Trenberth, K.; Karl, T.R.; Xie, S.-P.; Nieves, V.; Tung, K.-K.; Roemmich, D. The global warming hiatus: Slowdown or redistribution?. *Earth's Future*, **2016**, *4*, 472-482, DOI 10.1002/2016EF000417.
5. Yoshimura, S. *Limnology*; Sanseido, Tokyo, 1937; 520pp.
6. Boehrer, B.; Fukuyama, R.; Chikita. K.A. Stratification of very deep, thermally stratified lakes. Geophys. Res. Let., **2008**, 35, L16405, DOI 10.1029/2008GL034519.
7. Boehrer, B.; Fukuyama, R.; Chikita, K.A.; Kikukawa, H. Deep water stratification in deep caldera lakes Ikeda, Towada, Tazawa, Kuttara, Toya and Shikotsu. *Limnology*, **2009**, 10, 17-24.
8. Aihara, M.; Chikita, K.A.; Momoki, Y.; Mabuchi, S. A physical study on the thermal ice ridge in a closed deep lake: Lake Kuttara, Hokkaido, Japan. *Limnology*, **2010**, 11, 125-132.
9. Sakamoto, H. (the Bear Museum, Noboribetsu, Hokkaido, Japan). Personal communication, 2016.
10. Ashton, G.D. *River Lake Ice Engineering*. Water Resources Publications, LLC, 1986, 489pp
11. Gebre, S.; Boissy, T.; Alfredsen, K. Sensitivity of lake ice regimes to climate change in the Nordic region. *The Cryosphere*, **2014**, 8, 1589–1605.
12. Lepparanta, M. *Freezing of lakes and the evolution of their ice cover*. Springer, 2015, 361pp.
13. Saloranta, T.M.; Andersen, T. MyLake—A multi-year lake simulation model code suitable for uncertainty and sensitivity analysis simulations. *Ecological Modelling*, **2007**, 207, 45–60.
14. Nakao, K.; Otsuki, S.; Tanoue, R.; Naruse, R. Watershed leakage from the closed lake- Lake Kuttara. *Geophysical Bulletin of Hokkaido Universit*y, **1967**, 17, 47-64.
15. Chikita, K.; Hosogawa, Y.; Natsume, S. The characteristics of internal waves in a caldera lake introduced from field measurements: Lake Kuttara, Hokkaido. *Japanese Journal of Limnology*, **1993**, 54, 213-224.
16. Nakao, K. A hydrological study on the stability of water-level of a lake or a swamp. *Geophysical Bulletin of Hokkaido University*, **1971**, 25, 25-87.
17. Chen, C.-T. A.; Millero, F. J. Precise thermodynamic properties for natural waters covering only the limnological range. *Limnol. Oceanogr*., **1986**, 31, 657–662.
18. Goto, Y.; Johmori, A. Internal Structure of Kuttara Caldera, Hokkaido, Japan. *Bulletin of the Volcanological Society of Japan*, **2015**, 60, 35-46.
19. Boehrer, B.; Fukuyama, R.; Chikita, K.A. Geothermal heat flux into deep caldera lakes Shikotsu, Kuttara, Tazawa and Towada. *Limnology*, **2013**, 14, 129-134.
20. Brandt, R.E.; Warren, S.G. Surface albedo of the Antarctic sea ice zone. *Journal of Climate*, **2005**, 18, 3606-3622.
21. Kondo, J. *Meteorology in aquatic environments.* Asakura Publ., Ltd., Tokyo, 1994, 350pp.
22. Chikita, K.A.; Oyagi, H.; Yamane, S.; Aiyama, T., Itaya, T.; Okada, M.; Sakamoto, H. Thermal response of a temperate deep lake to climate change: Lake Kuttara, Hokkaido. *Journal of Japanese Association of Hydrological Sciences*, 2017, **47**, 73-86.